Volume 1
Number 1
January 2022
Pages 1–206

Sensors & Diagnostics

rsc.li/sensors

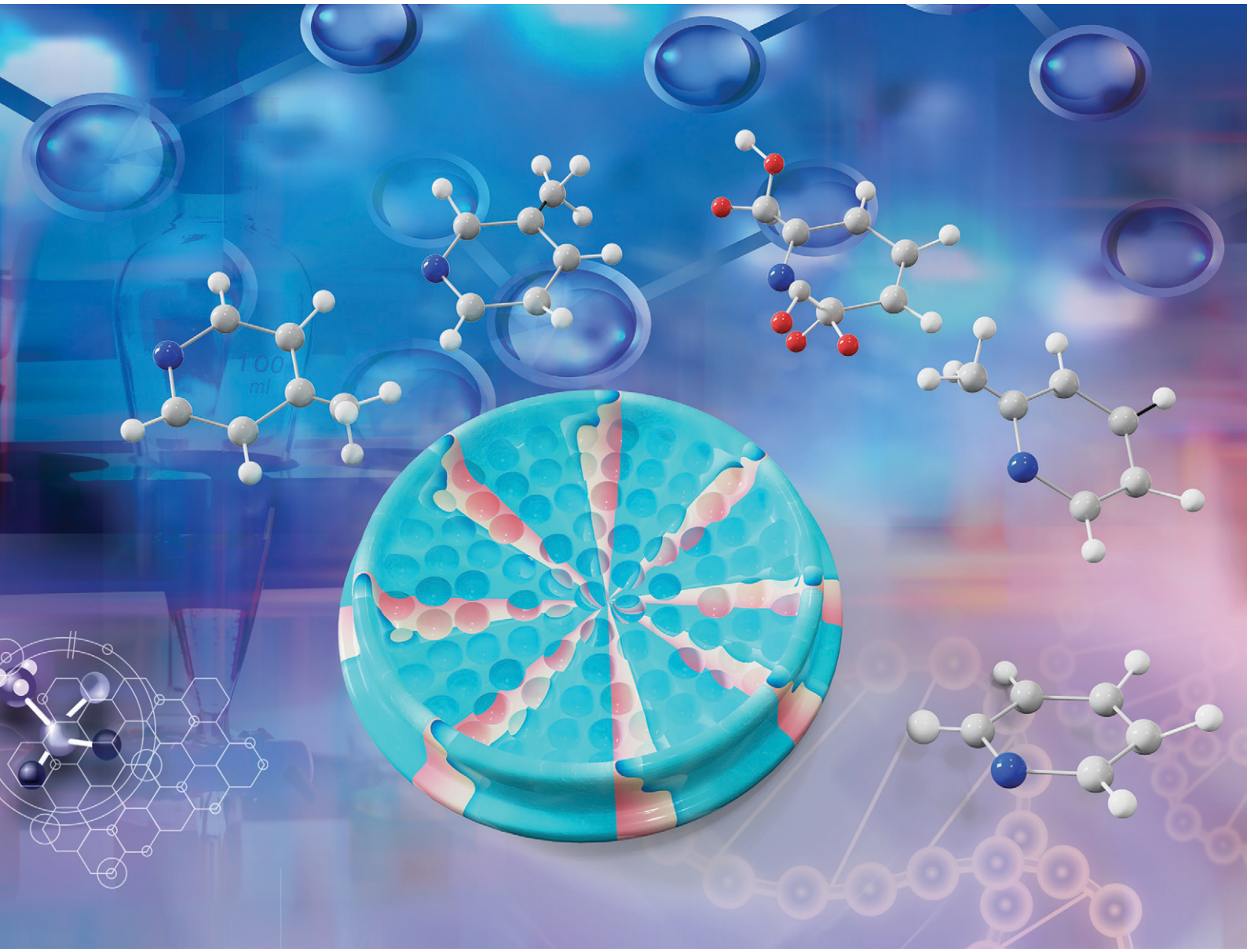

ISSN 2635-0998

ROYAL SOCIETY OF CHEMISTRY

COMMUNICATION

Quan Liu *et al.*

Highly improved performance of a film-based fluorescent sensor *via* a nanomesh scaffold strategy

Sensors & Diagnostics

ROYAL SOCIETY OF CHEMISTRY

COMMUNICATION

View Article Online
View Journal | View Issue

Cite this: *Sens. Diagn.*, 2022, **1**, 130

Received 3rd September 2021,
Accepted 14th October 2021

DOI: 10.1039/d1sd00016k

rsc.li/sensors

Highly improved performance of a film-based fluorescent sensor *via* a nanomesh scaffold strategy†

Quan Liu, *[ab] Meng Liu,[a] Dong Li,[a] Kun Li,[a] Haitao Xu,[a] Jiufu Lu,[a] Xianzhao Shao[a] and Taihong Liu [c]

Public safety and environmental monitoring are of great significance to maintain human health. Therefore, a simple and effective strategy for preparing the substrate layer of a film-based fluorescent sensor is developed by a nanomesh scaffold technology. The limit of detection of the nanomesh scaffold-modified sensor ranges from 4.8 ppb to 3750 ppm. This can provide an effective method for detecting potential biological warfare agent, 2,6-dicarboxyridine.

Film-based fluorescent sensing technology is mainly realized through the interaction between the analyte and fluorescent molecules in the excited state.[1] It has attracted wide attention due to its high sensitivity, good selectivity, easy device, miniaturization, and reusability.[2] More importantly, film-based fluorescent sensors can also be manufactured in a roll-to-roll manner, which enables the combination of different sensing modes to be used in one array. Film-based fluorescent sensors are a promising candidate to meet the requirements of complex samples and high-throughput detection.[3] These sensors have potential application value in the fields of complex samples and high-throughput detection, such as breath diagnosis, explosive detection, drug detection, indoor environment monitoring and precision agriculture.[4]

Using sensing molecules with specific response is one of the main strategies to prepare new film-based fluorescent sensors. A large number of research studies have focused on the structure and property study of fluorescent molecules.[5] The other important strategy is to change or modify the substrate structure used in the film-based fluorescent sensing. Fang *et al.* found that the sensing performance could be adjusted by changing the substrate of different materials. They used a pyrene bisimide (PBI) derivative as a fluorescent active substance to detect illegal drugs.[6] They found that the fluorescence intensity significantly quenched when using an ordinary smooth glass plate and polyvinyl chloride plate as the substrate. When a silica gel plate was used as the substrate, the fluorescent intensity of the film hardly changed in the presence of drug vapor. This shows that different substrate structures have huge impact on the sensing performance. Cheng *et al.* used ordered assembly arrays of zinc oxide (ZnO) nanorods as a film-based fluorescent sensing substrate to detect triacetone triperoxide (TATP) explosives.[7] Compared with the planar substrate, the ordered assembly arrays of ZnO nanorods improve the mass transfer of the analyte, resulting in significantly enhanced fluorescence emission, improved quenching efficiency and extended service life.

The above-mentioned examples clearly illustrate that the diffusion and adsorption speed of the analyte in the substrate directly affect the interaction between the analyte and the fluorescent molecule. The specific mass transfer process can be simulated by the theoretical model shown in Scheme 1a. In the process of film-based fluorescent sensing, VOCs will first diffuse to the surface of the film, and then adsorb on the surface of the film, affecting the fluorescence properties of fluorescent active substances. VOC molecular

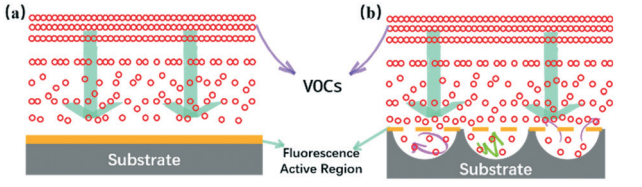

Scheme 1 Schematic of the VOC mass transfer process at the interface of the ground glass-based sensor (a) and the nanomesh scaffold modified sensor (b).

[a] *Shaanxi Province Key Laboratory of Catalytic Foundation and Applications, School of Chemical and Environmental Science, Shaanxi University of Technology, Hanzhong 723001, P. R. China. E-mail: liuq@sunt.edu.cn*
[b] *Key Laboratory of Organic Synthesis of Jiangsu Province, College of Chemistry, Chemical Engineering and Materials Science, Soochow University, Suzhou, 215123, P. R. China*
[c] *Key Laboratory of Applied Surface and Colloid Chemistry of Ministry of Education, School of Chemistry and Chemical Engineering, Shaanxi Normal University, Xi'an 710062, P. R. China*

† Electronic supplementary information (ESI) available. See DOI: 10.1039/d1sd00016k

diffusion flux plays a major role in the sensing process. Larger the diffusion flux is, higher the mass transfer efficiency will be, which indicates that the contact probability between fluorescent molecules and VOCs will be significantly improved, thus improving the sensing performance.[8] Referring to the Fang's group previous research reports by constructing non-planar porous structures to improve the diffusion flux.[9] We consider designing of the substrate layer has a bowl cavity can effectively to support fluorescent molecules on the surface (Scheme 1b), the maximum enhances fluorescence molecular contact area, at the same time ensure VOCs in longitudinal diffusion under the condition of constant flux, using fluorescent molecules at the bottom of the cavity further upward diffusion flux formation, the overall ascension VOCs response sensitivity.

In this report, the nanomesh scaffold technology was used to prepare a film-based fluorescence sensing substrate with an ordered bowl cavity substrate layer.[10] The nanomesh scaffold-modified film-based fluorescent sensor can be fabricated as per Scheme 2. The specific preparation steps can be seen in the Supporting Information. First, polystyrene (PS) spheres with a diameter of 300 nm were dispersed on the liquid surface to obtain PS colloidal sphere monolayer templates. The PS monolayer was transferred to a round glass substrate (Fig. 1a), and then the spin-coating method was used to fill silica gel into the void of the glass substrate covered by a PS sphere monolayer on the surface. It is worth noting that the bowl cavity with different hole depths can be prepared by selecting different concentrations of silica gel. Then, the substrate was immersed in a toluene solution to dissolve the PS sphere templates and endow the substrate with bowl-like cavity (Fig. 1b, S1 and S2†). Compared with the traditional ground glass-base substrate (Fig. S6†), the nanomesh scaffold-modified substrate with a neat and orderly microstructure is conducive to the mass transfer process of VOCs.

Due to the good photophysical properties of PBI, *N*,*N*′-bis(2-ethylhexyl)-1-bromoperylene-3,4,9,10-tetracarboxylic acid diimide (PBI–Br) was synthesized and selected as the fluorescent active material.[11] The synthesis and preparation of one-dimensional assembly of PBI–Br can be seen in the Supporting Information. The assembled PBI–Br was transferred to the nanomesh scaffold substrate surface to obtain the film-based fluorescent sensor. As shown in Fig. 1c and d, it is apparent that the PBI–Br assembly is evenly distributed on the surface of the nanomesh scaffold-modified substrate.

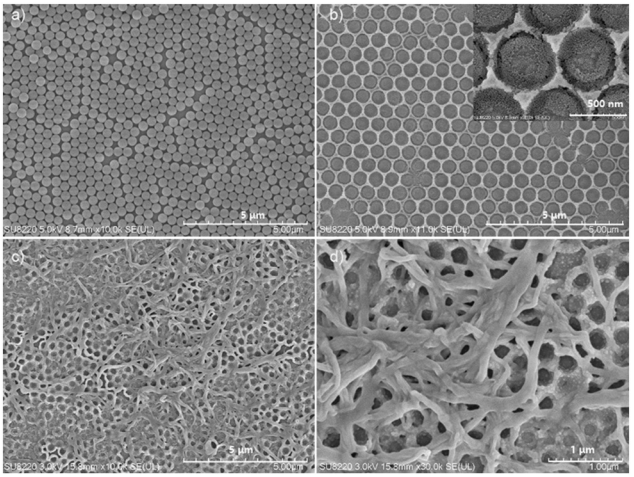

Fig. 1 SEM images of (a) the PS monolayer colloidal sphere templates (scale bar = 5 μm); (b) SiO_2 cavities on the glass substrate (scale bar = 5 μm), insets are enlarged views of SiO_2 cavities (scale bar = 500 nm); (c) assembly of PBI–Br was transferred to the surface of the SiO_2nanomesh scaffold-modified substrate (scale bar = 5 μm); (d) enlarged views of the nanomesh scaffold-modified sensor (scale bar = 1 μm).

Pyridine derivatives, common environmental pollutants in daily life, were selected as the detection object to evaluate the sensing performance.[12] The home-made sensing platform was used according to the protocol reported previously.[13] The detailed experimental procedures can be seen in the ESI.†

As we all know, the film thickness has a great influence on the sensing performance. Two kinds of the nanomesh scaffold-modified substrate with different hole depths (200 nm and 300 nm) were obtained by optimizing the concentration of silica gel. Pyridine and its derivatives (2-picoline, 3-picoline and 4-picoline) were diluted to the same concentration for the sensing test. The sensing results show that the substrate layer with deeper holes has higher response intensity, which may be due to the deeper holes more effectively improving the diffusion flux of VOCs (Fig. S9†). Therefore, the nanomesh scaffold-modified substrate with a greater hole depth (300 nm) was selected for further sensing experiments. Also, it was found that the nanomesh scaffold-modified sensor had more sensitive response intensity than the ground glass-based sensor (Fig. S7 and S8†). Specifically, the responses intensity of the nanomesh scaffold-modified sensor towards pyridine and its derivatives increased by 180% to 250% (Fig. 2).

Notably, the nanomesh scaffold-modified sensor can sense biomarker of anthrax spores (2,6-dicarboxyridine, PDA), which is a highly lethal agent to human beings and animals and also potential biological warfare agents.[14] The nanomesh scaffold-modified sensor has a significant response towards

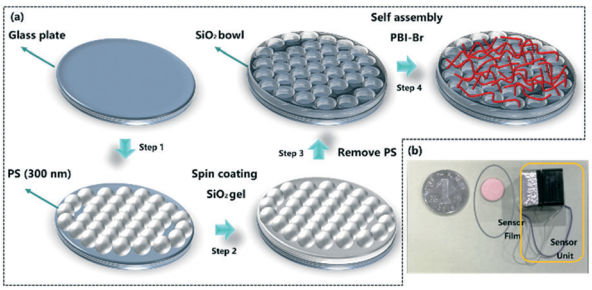

Scheme 2 (a) Schematic of the procedures for fabricating nanomesh scaffold-modified film-based fluorescent sensor; (b) physical drawing of the sensor and sensing unit.

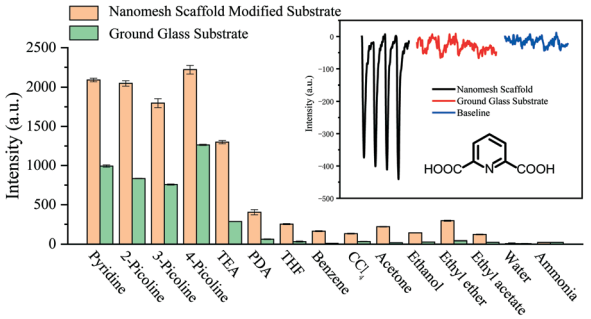

Fig. 2 Selectivity tests of the nanomesh scaffold-modified sensor and ground glass-based sensor to various pyridine derivatives and common solvent vapors. THF = tetrahydrofuran. Inset: the response intensity of the nanomesh scaffold-modified sensor and ground glass-based sensor towards saturated 2,6-dicarboxyridinevapor conducted at 25 °C.

saturated vapor of PDA (c_{PDA} = 2.8 ppt), and the response intensity is seven times stronger than that of the ground glass-based sensor (inset of Fig. 2). The simulated field tests were carried out for evaluating the practical applicability of the nanomesh scaffold-modified sensor (Fig. S10†). The results show that the sensor can detect PDA accurately.

The limit of detection (LOD) and stability of the nanomesh scaffold-modified sensor were further tested (Fig. 3a). The pyridine saturated vapor was diluted to different concentrations and injected to the sensor chamber to test the response intensity. It can be seen that the LOD of the nanomesh scaffold-modified sensor for pyridine ranges from 4.8 ppb to 3750 ppm. The nanomesh scaffold-modified sensor can detect the concentration of pyridine to as low as 4.8 ppb, which is lower than that of the glass-based sensor (24 ppb) (Fig. S11a†). By comparing with the reported literature (Table S1†), it is found that the sensor reported in this study has the lowest detection limit for pyridine.

The excellent re-usability of the nanomesh scaffold-modified sensor was proved by the results from more than 50 cycles of continuous tests with pyridine ($c_{pyridine}$ = 3750 ppm) (Fig. 3b). In addition, the signal strength of the nanomesh scaffold-modified sensor did not show significant attenuation after 4 h of continuous testing. This shows that the nanomesh scaffold-modified sensor has good photochemical stability. Compared with the glass substrate sensor, the nanomesh scaffold-modified sensor has less observable attenuation for both the reversibility and signal intensity (Fig. S11b†).

To distinguish the pyridine and its derivatives is of great practical significance for the specific detection of a certain target. Based on this, the sensors based on different substrates (with 200 nm and 300 nm hole depths and glass) are combined into the sensing array, and the distinguish detection can be realized through pattern recognition algorithm (PCA) of the response signal difference. As shown in Fig. 4a, the hot plots of the response intensities of the film-based devices towards pyridine and its derivatives resulted in an easily distinguishable pattern. Further, PCA is used to analyze the response signals of pyridine and its derivatives in different sensors (Fig. 4b). The PCA score plot as generated shows a clear clustering of the data using the first principal component (PC1) and the second principal component (PC2), where PC1 carries about 93.17% of the variance and PC2 carries 6.68%, demonstrating the strong discriminating capability of the nanomesh scaffold-modified sensor array.

Conclusions

A new type of film-based fluorescent sensor was constructed by the nanomesh scaffold technology. This technology is conducive to the contact between analytes and fluorescent molecules, which greatly improves the diffusion flux. The LOD of the nanomesh scaffold-modified sensor for pyridine ranges from 4.8 ppb to 3750 ppm. In particular, the nanomesh scaffold-modified sensor can be applied to detect PDA, a high-risk biological warfare agent. More importantly, this strategy can easily form a sensing array to realize distinguish detection of pyridine and its derivatives. It is expected to be an ideal choice for the detection and analysis of trace chemicals in public safety and environmental monitoring in the future.

We thank the Natural Science Basic Research Program of Shaanxi (2021KJXX-52), the Open Fund of Key Laboratory of

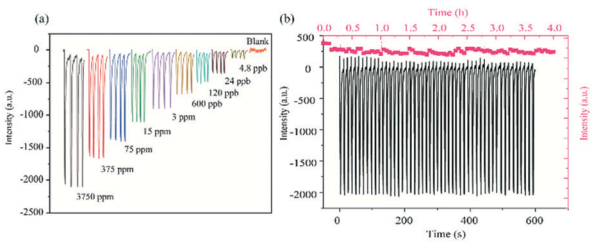

Fig. 3 (a) Signal intensity of the nanomesh scaffold-modified sensor recorded at different pyridine concentrations (varying from 4.8 ppb to 3750 ppm, 25 °C); (b) reusability and photochemical stability test of the nanomesh scaffold-modified sensor towards pyridine vapor ($c_{pyridine}$ = 3750 ppm, 25 °C).

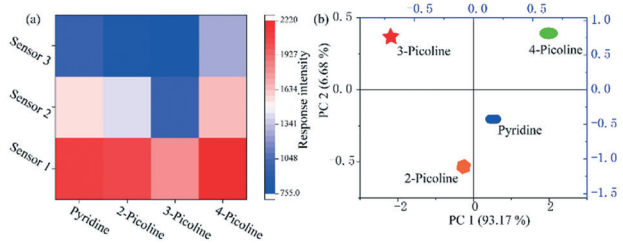

Fig. 4 (a) Hot plot of the response intensity of three sensors on exposure to pyridine and its derivatives (2-picoline, 3-picoline and 4-picoline), sensor 1 and sensor 2 was based on the nanomesh scaffold-modified substrate with 300 nm and 200 nm hole depths, sensor 3 was based on the ground glass substrate. (b) Two-dimensional PCA score plot for discriminating the saturated vapor of pyridine and its derivatives at 293 K *via* utilization of the response intensity of three sensors.

Organic Synthesis of Jiangsu Province (KJS2010), the Key Research and Development Program of Shaanxi (2020FP-026) and the Scientific Research Plan Projects of Shaanxi Education Department (20JS014).

Conflicts of interest

There are no conflicts to declare.

Notes and references

1 S. Chen, P. Slattum, C. Wang and L. Zang, *Chem. Rev.*, 2015, **115**, 11967–11998.
2 R. Miao, J. Peng and Y. Fang, *Langmuir*, 2017, **33**, 10419–10428.
3 Q. Liu, T. Liu and Y. Fang, *Langmuir*, 2020, **36**, 2155–2169.
4 (*a*) X. Jiang, H. Gao, X. Zhang, J. Pang, Y. Li, K. Li, Y. Wu, S. Li, J. Zhu, Y. Wei and L. Jiang, *Nat. Commun.*, 2018, **9**, 3799; (*b*) A. Jalal, F. Alam, S. Roychoudhury, Y. Umasankar, N. Pala and S. Bhansali, *ACS Sens.*, 2018, **3**, 1246–1263; (*c*) Y. Fu, W. Xu, Q. He and J. Cheng, *Sci. China: Chem.*, 2015, **35**, 3–15; (*d*) T. Minami, N. A. Esipenko, A. Akdeniz, B. Zhang, L. Isaacs and P. Anzenbacher, *J. Am. Chem. Soc.*, 2013, **135**, 15238–15243; (*e*) Z. Jiao, Y. Zhang, W. Xu, X. Zhang, H. Jiang, P. Wu, Y. Fu, Q. He, H. Cao and J. Cheng, *ACS Sens.*, 2017, **2**, 687–694; (*f*) D. Sun, L. Huang, H. Pu and J. Ma, *Chem. Soc. Rev.*, 2021, **50**, 1070–1110.
5 F. Wurthner, C. R. Saha-Moller, B. Fimmel, S. Ogi, P. Leowanawat and D. Schmidt, *Chem. Rev.*, 2016, **116**, 962–1052.
6 K. Liu, C. Shang, Z. Wang, Y. Qi, R. Miao, K. Liu, T. Liu and Y. Fang, *Nat. Commun.*, 2018, **9**, 1695.
7 (*a*) C. He, D. Zhu, Q. He, L. Shi, Y. Fu, D. Wen, H. Caoand and J. Cheng, *Chem. Commun.*, 2012, **48**, 5739–5741; (*b*) D. F. Zhu, Q. Chen, Y. Y. Fu, C. He, L. Q. Shi, X. Meng, C. M. Deng, H. M. Cao and J. G. Cheng, *ACS Nano*, 2011, **5**, 4293–4299.
8 K. Luan, R. Meng, C. Shan, J. Cao, J. Jia, W. Liu and Y. Tang, *Anal. Chem.*, 2018, **90**, 3600–3607.
9 (*a*) H. Peng, L. Ding, T. Liu, X. Chen, L. Li, S. Yin and Y. Fang, *Chem. – Asian J.*, 2012, **7**, 1576–1582; (*b*) G. Wang, X. Chang, J. Peng, K. Liu, K. Zhao, C. Yu and Y. Fang, *Phys. Chem. Chem. Phys.*, 2015, **17**, 5441–5449; (*c*) M. He, H. Peng, G. Wang, X. Chang, R. Miao, W. Wang and Y. Fang, *Sens. Actuators, B*, 2016, **227**, 255–262; (*d*) J. Zhang, K. Liu, Z. Liu, Z. Wang, C. Hua, T. Liu and Y. Fang, *ACS Appl. Mater. Interfaces*, 2021, **13**, 5625–5633; (*e*) Y. Qi, W. Xu, N. Ding, X. Chang, C. Shang, H. Peng, T. Liu and Y. Fang, *Mater. Chem. Front.*, 2019, **3**, 1218–1224.
10 (*a*) X. Zhong, E. Pavlica, S. Li, A. Klekachev, G. Bratina, T. Ebbesen, E. Orgiu and P. Samori, *Nat. Nanotechnol.*, 2016, **11**, 900–906; (*b*) L. Zhang, E. Pavlica, X. Zhong, F. Liscio, S. Li, G. Bratina, E. Orgiu and P. Samori, *Adv. Mater.*, 2017, **29**, 1605760; (*c*) C. Gu, N. Hosono, J. Zheng, Y. Sato, S. Kusaka, S. Sakaki and S. Kitagawa, *Science*, 2019, **363**, 387–391.
11 Z. Zhou, W. Xiong, Y. Zhang, D. Yang, T. Wang, Y. Che and J. Zhao, *Anal. Chem.*, 2017, **89**, 3814–3818.
12 (*a*) G. G. Huang, C. J. Lee, J. Yang, C. H. Chang, M. Sathiyendiran, Z. Z. Lu and K. L. Lu, *ACS Appl. Mater. Interfaces*, 2016, **8**, 35634–35640; (*b*) W. Chen, S. A. Elfeky, Y. Nonne, L. Male, K. Ahmed, C. Amiable, P. Axe, S. Yamada, T. D. James, S. D. Bull and J. S. Fossey, *Chem. Commun.*, 2011, **47**, 253–255; (*c*) Y. Xie, W. Cheng, B. Jin, C. Liang, Y. Ding and W. Zhang, *Analyst*, 2018, **143**, 5583–5588; (*d*) S. Soorkia, C. A. Taatjes, D. L. Osborn, T. M. Selby, A. J. Trevitt, K. R. Wilsone and S. R. Leonew, *Phys. Chem. Chem. Phys.*, 2010, **12**, 8750–8758.
13 Z. Wang, G. Wang, X. Chang, K. Liu, Y. Qi, C. Shang, R. Huang, T. Liu and Y. Fang, *Adv. Funct. Mater.*, 2019, **29**, 1905295.
14 L. Liu, W. Xiong, L. Cui, Z. Xue, C. Huang, Q. Song, W. Bai, Y. Peng, X. Chen, K. Liu, S. Zhang, L. Wen, Y. Che and T. Wang, *Angew. Chem.*, 2020, **59**, 15953–15957.